The Crystal Structure of the Actin Binding Domain from α-Actinin in its Closed Conformation: Structural Insight into Phospholipid Regulation of α-Actinin

ARTICLE *in* JOURNAL OF MOLECULAR BIOLOGY · MAY 2005

Impact Factor: 4.33 · DOI: 10.1016/j.jmb.2005.01.002 · Source: PubMed

4 AUTHORS, INCLUDING:

Kristina Djinović-Carugo
University of Vienna
114 PUBLICATIONS **3,391** CITATIONS

doi:10.1016/j.jmb.2005.01.002 J. Mol. Biol. (xxxx) xx, 1–15

JMB

Available online at www.sciencedirect.com

SCIENCE DIRECT®

ELSEVIER

The Crystal Structure of the Actin Binding Domain from α-Actinin in its Closed Conformation: Structural Insight into Phospholipid Regulation of α-Actinin

Giacomo Franzot[1,2], Bjoern Sjoeblom[1,3], Mathias Gautel[3]* and Kristina Djinović Carugo[1,3]*

[1]*Structural Biology Laboratory Elettra-Sincrotrone Trieste in Area Science Park, S.S. 14 Km 163,5 34012 Trieste, Italy*

[2]*Max F. Perutz Laboratories University Departments at Vienna Biocenter, Institute for Theoretical Chemistry and Molecular Structural Biology University of Vienna, Campus Vienna Biocenter 6/1, Rennweg 95b, A-1030 Vienna, Austria*

[3]*Muscle Cell Biology, The Randall Division for Cell and Molecular Biophysics and Cardiovascular Division New Hunt's House, King's College London, Guy's Campus London SE1 1UL, UK*

**Corresponding authors*

α-Actinin is the major F-actin crosslinking protein in both muscle and non-muscle cells. We report the crystal structure of the actin binding domain of human muscle α-actinin-3, which is formed by two consecutive calponin homology domains arranged in a "closed" conformation. Structural studies and available biochemical data on actin binding domains suggest that two calponin homology domains come in a closed conformation in the native apo-form, and that conformational changes involving the relative orientation of the two calponin homology domains are required for efficient binding to actin filaments. The actin binding activity of muscle isoforms is supposed to be regulated by phosphatidylinositol 4,5-bisphosphate (PtdIns(4,5)P_2), which binds to the second calponin homology domain. On the basis of structural analysis we propose a distinct binding site for PtdIns(4,5)P_2, where the fatty acid moiety would be oriented in a direction that allows it to interact with the linker sequence between the actin binding domain and the first spectrin-like repeat, regulating thereby the binding of the C-terminal calmodulin-like domain to this linker.

Keywords: α-actinin; actin binding domain; calponin homology domain; actin filaments; skeletal muscle

Introduction

The cytoskeleton consists of a number of filamentous systems composed of polymers of actin, tubulin and intermediate filament proteins. These proteins form the filaments of actin stress fibers, microtubules and intermediate filaments. Their filamentous state provides the cell with networks of structures that are highly dynamic as well as highly stable. These networks give the cell internal scaffolds for maintaining and modelling cell shape and provide routes for inter- and intracellular traffic and signalling. An important family of cytoskeleton proteins are those that crosslink or bundle actin filaments (α-actinin, filamin, and fimbrin) or link the actin filaments to the cell membrane (β-spectrin, dystrophin and utrophin) or other filamentous systems (plectin). The common functional domain of these proteins is the actin binding domain (ABD).

α-Actinin is the major F-actin crosslinking protein in both muscle and non-muscle cells.[1] α-Actinin is a functional antiparallel homodimer and is composed of an N-terminal ABD, followed by a rod domain consisting of four spectrin-like (SR) repeats and a C-terminal calmodulin-like (CaM) domain. The actin binding domain (ABD) consists of two consecutive calponin homology (CH) domains.[2] Several α-actinin isoforms exist,[3] which are regulated differently: actin binding in the non-muscle isoforms is Ca^{2+}-sensitive, whereas in muscle α-actinin it is not.[4] The CaM domain consists of two EF-hand motifs. The CaM domain of the non-muscular isoforms can bind Ca^{2+} and thereby regulate the actin binding activity. The CaM domain of the

Abbreviations used: PtdIns(4,5)P_2, phosphatidylinositol 4,5-bisphosphate; ABD, actin binding domain; CaM, calmodulin-like; CH, calponin homology.

E-mail addresses of the corresponding authors: mathias.gautel@kcl.ac.uk; kristina.djinovic@univie.ac.at

muscle isoforms does not bind Ca^{2+} and their activity is Ca^{2+}-insensitive. The actin binding activity of muscle isoforms might instead be regulated by phosphatidylinositol 4,5-bisphosphate ($PtdIns(4,5)P_2$), and the binding site was mapped to a region of the second CH domain in ABD.[5] This region is also involved in the regulated interaction of the CaM domain with titin.[6]

Apart from its interaction with actin, α-actinin has emerged as a major multivalent platform mediating interactions with many cytoskeletal or regulatory proteins.[7,8] At the membrane, in focal adhesions and cell–cell contacts, α-actinin interacts with capZ, vinculin, zyxin and cell surface receptors such as the NMDA or integrin receptors. Along the actin cytoskeleton, α-actinin interacts with signalling molecules such as the protein kinases MEKK1 and PKN, zinc-finger proteins like ALP, and PDZ domain proteins like ZASP/cypher.[7,9] In muscle, in addition to some of these proteins, the interactions with sarcomeric proteins are functionally possibly most important: α-actinin binds to the giant actin filament ruler titin and to the novel Z-disk proteins myotilin and ZASP.[9,10]

Striated muscle α-actinin, predominantly isoforms 2,[11] interacts with two classes of binding sites for the Z-disk portion of titin;[12] the highly homologous skeletal muscle-specific α-actinin-3 shows similar binding (Figure 1(a)). The titin Z-repeats provide multiple binding sites for the C-terminal CaM domain of α-actinin,[6] whose differential splicing appears to determine Z-disk thickness by determining the number of cross-links in this structure.[13,14] At the Z-disk periphery, a unique site interacts with the two central spectrin-like repeats of the α-actinin rod.[12] Controlled activation of protein–protein interactions is a major mechanism for the sequential integration of protein components into cytoskeletal structures also in muscle, and muscle α-actinin is accordingly regulated in a specific way. The interaction of muscle α-actinin with titin is regulated intrasterically by a phospholipid-dependent mechanism that controls its interaction with the titin,[6] and requires the presence of both CH domains for full regulation. However, no structural information on α-actinin ABDs is available so far that would allow us to analyse this regulation mechanism in atomic detail.

Three-dimensional structures of actin binding domains have been reported for the following actin binding proteins: plectin,[15–17] human fimbrin,[18] and fimbrins from *Arabidopsis thaliana* and *Schizosaccharomyces pombe*.[19] The structures of plectin and fimbrin ABD revealed two CH domains to be in intimate contact, and are therefore referred to as "closed" conformations. Interestingly, structural flexibility within ABD domains from two crystallographically independent fimbrin core molecules was observed: the CH1 domain undergoes a rotation of about 50° in these two molecules.[19] ABDs of utrophin and dystrophin assemble into antiparallel dimers, with the N-terminal CH1 of one monomer in close association with the C-terminal CH2 of the other. Each ABD monomer adopts an "open" conformation comprising the two CH domains connected by an α-helix.

In order to gain further insight into the molecular details of filamentous actin cross-linking structures in the muscle Z-disk, and the structural basis of phospholipid regulation *via* the actin binding domain, we determined the molecular structure of the actin binding domain of human skeletal muscle α-actinin (isoform 3) in two crystal forms.

Results and Discussion

Titin binding

Similar to α-actinin-2, the highly homologous α-actinin-3 was also found to show phospholipid-regulated binding to the titin Z-repeats. Binding could be stimulated by negatively charged phospholipids like phosphatidyl-inositol 4,5-bisphosphate ($PtdIns(4,5)P_2$) (Figure 1(a)) as well as by lysophosphatidic acid (not shown). No activation was observed by the phospholipid head groups alone, in agreement with earlier observations for α-actinin-2.[6]

This interaction is in agreement with the high level of amino acid sequence identity (>92%) of the binding regions in the ABD and CaM domain.[11] Figure 1(b) shows the amino acid sequence alignment of the N-terminal regions of human α-actinin isoforms 2 and 3.

Structure solution and refinement

The construct crystallised comprises amino acid residues 26–273 of human α-actinin-3, spanning the two CH domains in tandem and a 44 amino acid residue N-terminal extension. Two crystal forms (H and L), diffracting to 1.55 Å and 2.19 Å, respectively, were structurally characterised. The phase problem of form L was solved with molecular replacement techniques using the structure of the CH1 domain of utrophin,[16] and the CH2 domain from β-spectrin.[20] In the L form, residues 42–265 were clearly visible in the electron density maps, and refined to a final *R*-factor of 22.7% and a free *R*-factor of 27.3% for the diffraction data to 2.19 Å. The structure of form H was solved with molecular replacement techniques using the refined structure of form L as the search model. The structure was refined to 1.60 Å resolution with a final *R*-factor of 18.2% and a free *R*-factor of 20.8%, and consists of two ABD molecules per asymmetric unit: molecule A comprises residues 42–266 and molecule B comprises residues 42–268 of human skeletal muscle α-actinin-3. The pertinent refinement details along with the statistics for the final refined models are given in Table 1.

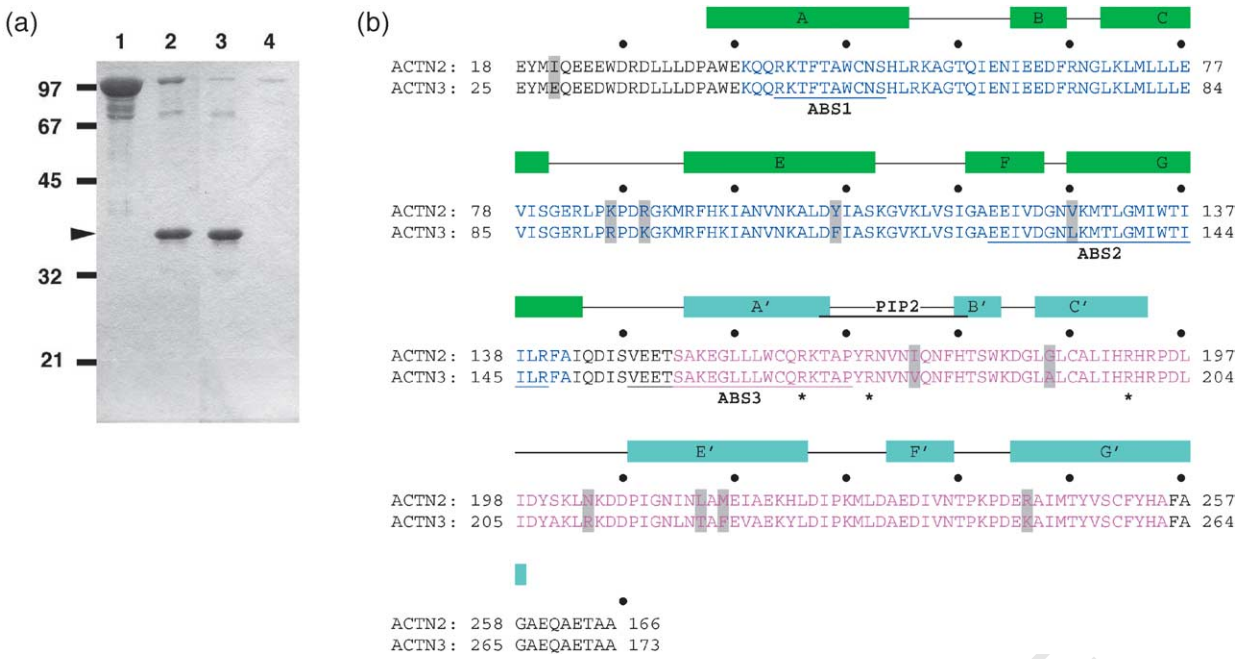

Figure 1 (a) and (b) (*legend next page*)

Structure of the ABD from striated muscle α-actinin

Superposition of three crystallographically independent ABD domains from two crystal forms, H and L, gives r.m.s. deviations for C^{α} atoms between molecules A and B of crystal form H of 0.34 Å, and between ABD in crystal form L and ABD of molecules A and B of crystal form H of 0.49 Å and 0.53 Å, respectively.

The structure of the ABD from α-actinin, in both crystal forms, can be described as a closed conformation, in which the CH1 and CH2 domains are in extensive contact (Figure 1(c) and (d)), similar to the conformation observed in plectin[15] and fimbrin.[18] Given that all the three ABD structures are

Table 1. Data collection and refinement statistics

	Form H	Form L
A. *Data collection*		
Wavelength (Å)	1.00	1.5418
Space group	*P*1	$P2_1$
Cell parameters		
a (Å)	38.5	46.31
b (Å)	45.96	38.54
c (Å)	66.70	65.48
α (deg.)	86.7	
β (deg.)	87.8	99.7
γ (deg.)	87.3	
Unique reflections	63,223	12,180
Resolution (Å)	1.55	2.19
Redundancy	1.9	2.8
Completeness %	95.2 (89.5)	97.4 (93.1)
R_{merge}	0.035 (0.307)	0.089 (0.186)
B. *Refinement*		
No. reflections	56,760	11,674
Resolution (Å)	1.60	2.19
R_{factor}	0.182	0.227
R_{free}	0.208	0.273
No. protein atoms	3626	1780
No. water molecules	459	193
r.m.s.d. from ideality		
Bond lengths (Å)	0.004	0.007
Bond angles (deg.)	1.1	1.10
Overall *B*-value (Å^2)	19.8	17.8

Numbers in parentheses refer to the last resolution shell. $R_{merge} = \Sigma|I_i - \langle I\rangle|/\Sigma I_i$, where I_i is the intensity of an individual reflection and $\langle I\rangle$ is the mean intensity of that reflection. $R_{factor} = \Sigma|F_o - F_c|/\Sigma F_o$. R_{free} is the cross-validation R_{factor} computed for the test set of reflections (6.7% and 10%, for forms H and L, respectively) which are omitted from the refinement process.

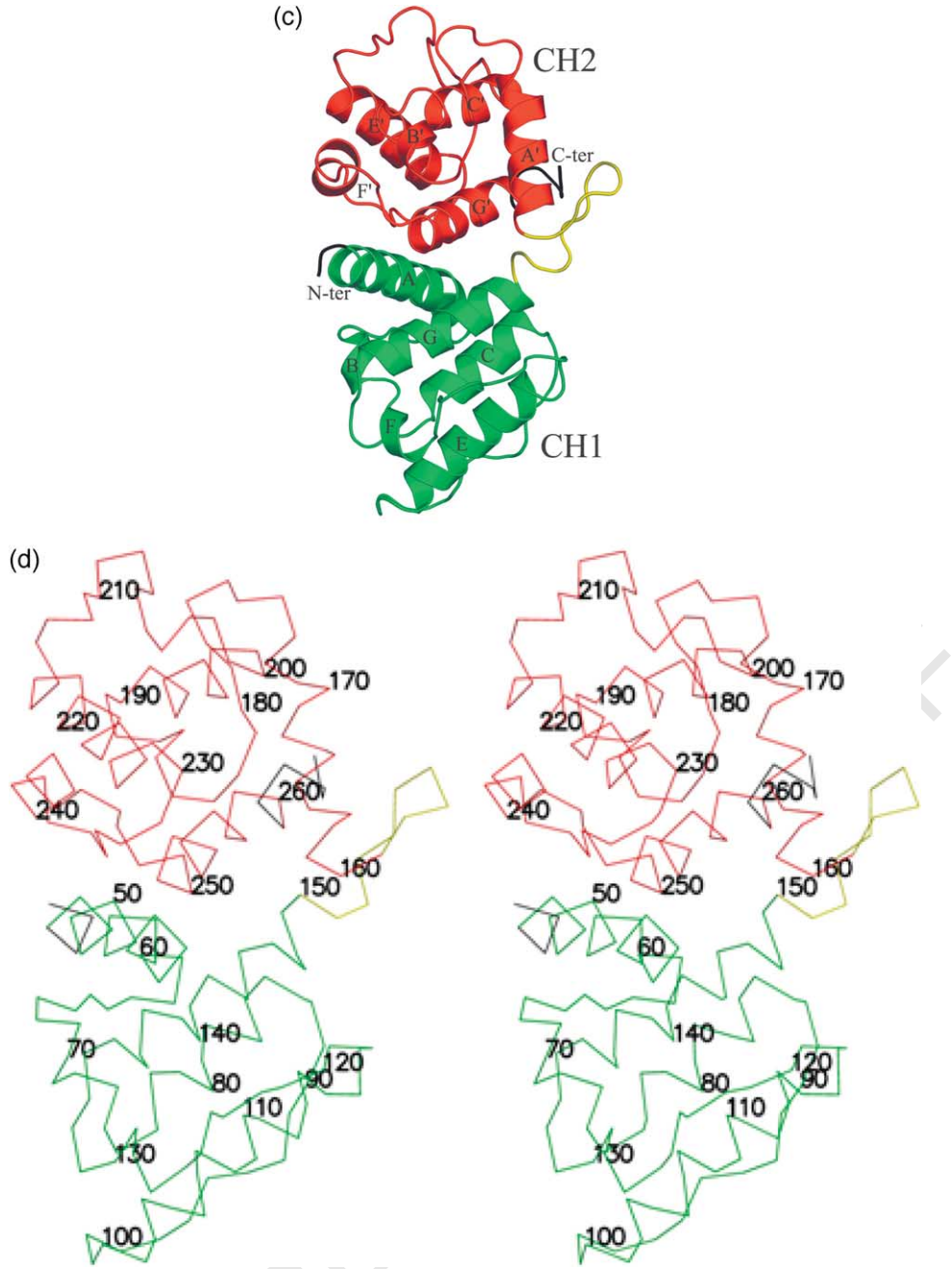

Figure 1. (a) Phospholipid regulated binding of α-actinin-3 to titin Zr7 in a GST-pulldown assay. Lane 1, α-actinin-3 input (10%). Lane 2, eluate of GST-Zr7 glutathione beads after incubation with α-actinin-3 in the presence of 25 μM PtdIns(4,5)P_2 showing binding of α-actinin to GST-Zr7. In the absence of phospholipid, binding was significantly reduced (lane 3) in comparison to background binding to glutathione beads (lane 4) or GST alone. Marker molecular masses are given in kDa; arrowhead, position of GST-Zr7. (b) Amino acid sequence alignment of N-terminal regions of human α-actinin isoforms 2 and 3 (ACTN2, (3). Residues belonging to the classical CH domain definition are shown in blue and magenta for CH1 and CH2 domains, respectively. Secondary structure elements are indicated by boxes and are labelled as in (c); the position of every tenth residue is indicated by dots. Sequence differences are highlighted, actin binding sites 1–3 are underlined, the PtdIns(4,5)P_2 binding site is marked with a line above, and the proposed PtdIns(4,5)P_2 ligands are marked with a star beneath. (c) Schematic view of the tertiary structure of the α-actinin ABD. CH1 and CH2 domains are coloured green and red, respectively, the loop connecting the two consecutive CH domains is coloured yellow. The amino acid residues that do not belong to the classical definition of the CH domain are depicted in black. α-Helices, as well as N and C termini are labelled. The Figure was prepared by PyMOL. (d) Stereo C^{α} trace of the ABD in the same orientation and colour code as in (b). The sequence is numbered every ten residues. The Figure was prepared by PyMOL (http://pymol.sourceforge.net).

essentially in identical closed conformations, we will refer to molecule A of the crystal form H.

Each individual CH domain is composed of four principal α-helices (A, C, E, and G) that form the core of the domain. Helices C and G are parallel with each other, sandwiched between N-terminal helix A, which forms an angle of 60° with the axis defined by the central two helices, and helix E at about 25° with respect to the same axis. Out of three minor helices (B, D and F) that are observed in the β-spectrin CH2 domain[20] only B and F are present in the α-actinin structure. Helix D, located in the long loop connecting the helices C and E is absent from all CH domains of α-actinin.

The two consecutive CH domains that form the complete actin binding domain (Figure 1(c)) have an extensive interface. The CH1 domain contributes to the interface with the N and C-terminal helices (A and G). The CH2 domain is in contact with the preceding domain *via* the E″–F″ loop connecting helices E″ and F″, and the two C-terminal helices F″ and G″. Helices A and G of the first domain form a groove, into which the C-terminal helix G″ of the consecutive CH2 domain packs tightly. Additionally, the connecting loop E″–F″ and the helix F″ of the CH2 domain are juxtaposed to helix A of the CH1 domain, forming in this way an extensive common interface. Of the interactions contributing to the interface, 61% are hydrophobic and form a network of van der Waals contacts. The area of interface is 880 Å^2 (13% of the solvent-accessible area of a CH domain). The complementarities between the surfaces in the domain interface can be evaluated by the gap index, which is defined as the ratio between the gap volume between the molecules (Å^3) and the solvent-accessible area at the interface (Å^2).[21] The gap index for the α-actinin domains is 1.70 Å. This parameter compares best with the corresponding parameter found in permanent heterocomplexes, which form together with enzyme–inhibitor complexes the most complementary interfaces.[21]

In α-actinin-3, an eight-residue linker connects the two CH domains in a stable hairpin conformation (Figure 1(c)). Its relative orientation towards the actin-binding region is stabilised by several interactions with N and C-terminal helices of the CH2 domain. The length of the linker between the two tandem CH domains ranges from eight residues, as in α-actinin, to up to 60 residues as observed in parvin, a representative of a novel family of small focal adhesion-associated proteins.[22] The molecular architecture of the ABD domain allows linkers of various lengths to be accommodated between two tandem CH domains without disturbing the overall structure of the actin-binding region, and without interfering with residues directly involved in binding to actin filaments.

ABD domains: open *versus* closed conformation

The ABD of α-actinin as reported here adopts the closed conformation in the crystal form L with one molecule per asymmetric unit as well as in the crystal form H, which hosts two molecules per asymmetric unit. Structural comparison of the α-actinin ABD with plectin (Figure 2(a); Table 2) and fimbrin (Table 2) gives an r.m.s. deviation of 1.46 Å (for 201 superimposable C^α atoms) and 1.79 Å, 1.84 Å and 1.86 Å (for 149, 120 and 138 superposable C^α atoms), for the proteins from *Homo sapiens*, *A. thaliana* and *S. pombe*, respectively. The molecules adopt a similar closed structure; the major differences reside in the lengths and conformation of connecting loops and, to a certain extent, in the relative orientation of CH domains in case of fimbrins, while the core structure of individual CH domains remains well preserved.

Structural superposition of the α-actinin ABD with a single utrophin ABD domain can be performed only on a pair-wise CH domain basis, and not over the whole molecule, since the two CH domains adopt markedly different relative orientations (Figure 2(b)). Overlays of 101 superposable C^α atoms of the CH1 domain give an r.m.s. deviation of 0.83 Å (Table 2). Similarly, when the CH2 domains of both molecules are compared, the r.m.s. deviation for 95 C^α atoms is 0.83 Å, indicating that the structural cores of both CH domains are well preserved in the two molecules. Major differences between the CH1 domains are in the lengths and conformations of the A–B loop, which connects the first two α-helices, and in the conformation of the linker between the tandem CH domains. While in the closed form of the α-actinin ABD the linker forms a hairpin structure, in the open utrophin conformation it continues the C-terminal helix and finishes as a sharp turn towards the consecutive CH domain. The CH2 domains differ mostly in the local conformation and position of helix B″ and conformation of the C″–D″ loop. The α-actinin ABD superposed on the utrophin dimer (Figure 2(b)) shows that quaternary arrangement of the utrophin dimer brings the CH1 of one monomer into contact with the CH2, to form a closed conformation as observed in the α-actinin ABD (r.m.s. deviation on 197 C^α atoms is 1.31 Å, Table 2). The conservation of the CH1–CH2 interface suggests that the utrophin ABD might adopt a compact structure in its monomeric form whereas the dimeric state is similar to that found in the crystal structure.

Similar structural comparisons were also performed for the dystrophin ABD monomer and dimer. The CH1 domains of α-actinin and dystrophin overlay with a r.m.s. deviation of 0.90 Å for 93 matching C^α atoms (Table 2), and the CH2 of dystrophin superposes with the corresponding moiety of α-actinin with an r.m.s. deviation of 0.80 Å for 96 C^α atoms. It is clear that the core of both CH domains is again highly preserved; the conformational differences reside in connecting loops and the linker between the two CH domains. Although the comparison of the dystrophin and utrophin dimers reveals a large conformational

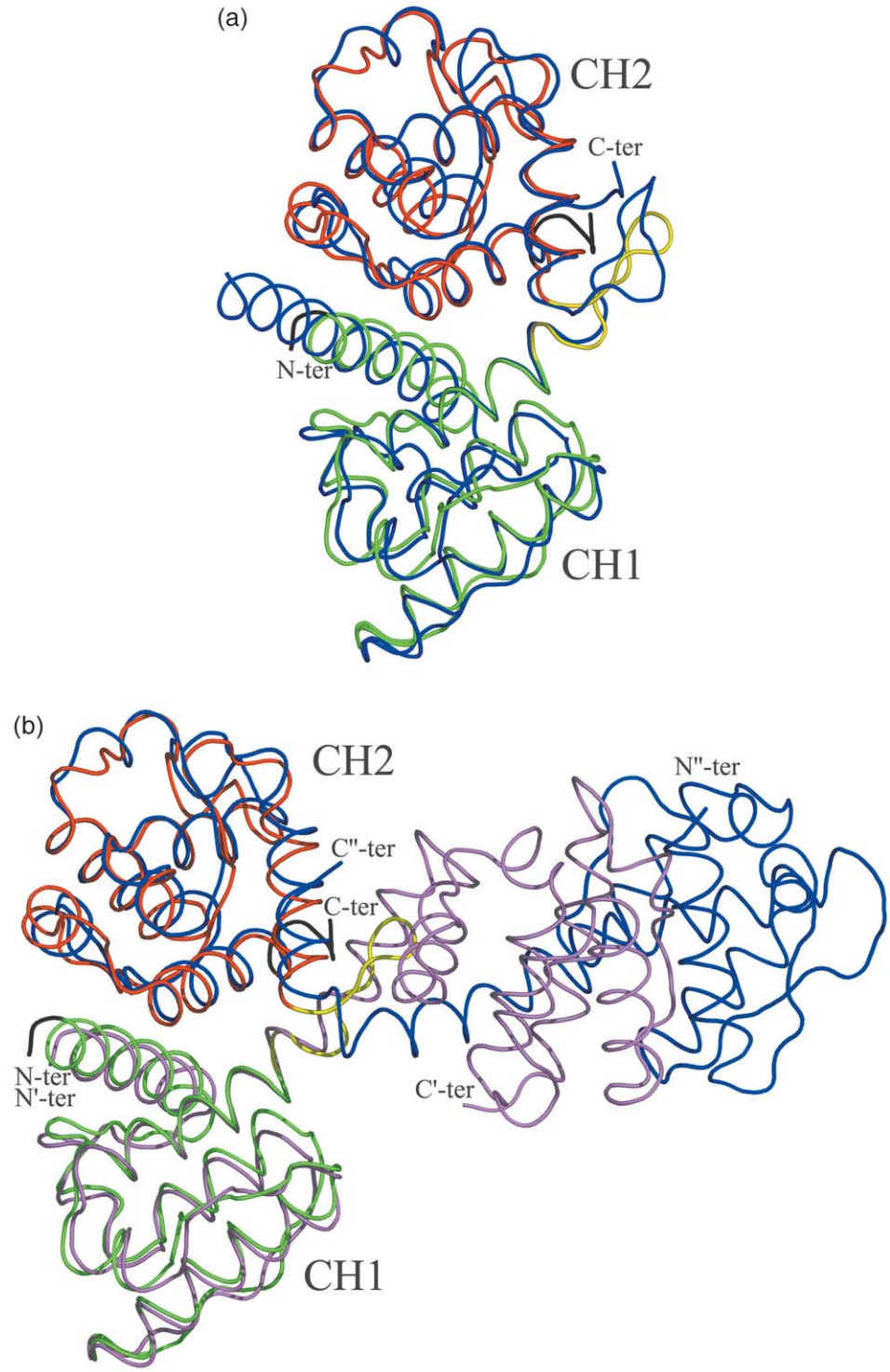

Figure 2. (a) Structural superposition of ABDs from α-actinin and plectin made by TOPP. The color code for ABD from α-actinin is as in Figure 1, plectin is shown in blue. The superimposed proteins are oriented according to Figure 1. The Figure was prepared by PyMOL. (b) Structural superposition of ABDs from α-actinin and utrophin was made by TOPP. The color code for ABD from α-actinin is as in Figure 1, utrophin subunits are shown in yellow and in blue. The superimposed proteins are oriented according to Figure 1. The Figure was prepared by PyMOL.

shift, transformation is a 72° rigid-body rotation of a CH1–CH2 pair (from different monomers) relative to the other pair, comparison of the α-actinin ABD with the dystrophin dimer again shows the conservation of the dimer interface formed by interactions between CH1 and CH2 domains that belong to two different subunits (the r.m.s. deviation for 191 C^{α} atoms is 1.53 Å).

ABDs from utrophin and dystrophin are monomeric in solution, but form dimers in the crystals. The pairing between CH1 and CH2 domains is very similar even though the two CH domains

Table 2. Structural comparisons of ABD and CH domains

Protein name	Pdb code	Sequence	Matching residues	Sequence identity (%)	r.m.s.d. (Å)
A. *ABD from α-actinin (residues 42–266, chain A, form H) compared to other ABDs*					
Dystrophin*	1DXX	9–240	191	47.1	1.53
Utrophin*	1QAG	31–256	197	45.2	1.31
Plectin	1MB8	175–400	201	51.7	1.46
Fimbrin (*H. sapiens*)	1AOA	118–372	149	22.8	1.79
Fimbrin (*A. thaliana*)	1PXY	124–371	120	25.0	1.84
Fimbrin (*S. pombe*)	1RT8	110–364	138	23.9	1.86
B. *CH1 from α-actinin (residues 45–149) compared to other CH1 domains*					
Dystrophin	1DXX	15–119	93	48.4	0.90
Utrophin	1QAG	31–135	101	42.6	0.83
Plectin	1MB8	179–282	102	53.9	0.75
Fimbrin (*H. sapiens*)	1AOA	120–236	79	26.6	1.38
Fimbrin (*A. thaliana*)	1PXY	124–242	82	20.7	1.43
Fimbrin (*S. pombe*)	1RT8	110–234	85	29.4	1.37
C. *CH2 from α-actinin (residues 158–261) compared to other CH2 domains*					
Dystrophin	1DXX	134–237	96	46.9	0.80
Utrophin	1QAG	150–252	95	47.4	0.83
Plectin	1MB8	295–397	95	50.5	0.83
Fimbrin (*H. sapiens*)	1AOA	264–372	67	20.9	1.27
Fimbrin (*A. thaliana*)	1PXY	268–371	77	26.0	1.39
Fimbrin (*S. pombe*)	1RT8	262–364	74	25.7	1.35
β-Spectrin	1BKR	173–275	99	59.6	0.67
D. *CH1 from α-actinin compared to CH domain of calponin*					
Calponin	1H67	28–131	74	16.2	1.68
E. *CH2 from α-actinin compared with CH domain of calponin*					
Calponin	1H67	28–131	74	19.7	1.66

originate from different polypeptide chains. The preservation of an interface between two domains whether in monomer or oligomer form is referred to as domain swapping,[23,24] which is often observed as a crystallization artefact.[25]

Whether the dimerization is simply a crystallographic artefact, or has functional significance with respect to actin binding was also addressed by several cryo-electron microscopy (cryo-EM) studies of ABDs with actin filaments. While the reconstruction of the fimbrin ABD with actin filaments was modelled on the closed conformation,[26] there is some controversy concerning whether the closed or open conformations are present when the utrophin or dystrophin ABD is bound to actin filaments.[27–30] The 3D reconstruction of α-actinin from chicken gizzards obtained by cryo-EM of frozen hydrated 2D arrays[31,32] also revealed a possible open bilobed structure associated with the open conformation of the actin binding domain. The cryo-EM reconstruction actin filaments decorated with α-actinin,[33] however, revealed a more globular difference density, suggesting that α-actinin might also associate with actin filaments in a more compact form such as that seen in our α-actinin crystal structure. In a recent reconstruction of the smooth muscle α-actinin by cryo-EM, the ABD was observed in both, open and closed conformations,[34] suggesting conformational variability that may be the basis of Ca^{2+} and PtdIns(4,5)P_2 regulation.

Structural evolution of CH domains

The structures of the CH domains from the L and H crystal forms of the α-actinin ABD were compared to all the known structures of CH domains (Table 1 of the Supplementary Data) by means of the PRIDE algorithm.[35]

It is well known that the CH domains can be clustered in distinct groups on the basis of their sequence relationships. The 3D structures of three of these types of CH domains have been characterized experimentally. There are seven 3D structures of CH domains of type 1 that have been structurally characterized, eight structures of CH domains of type 2 are known, and only one CH domain of type 3 has been determined insofar. These 16 crystal structures were compared with the PRIDE values, which monitors the similarity between pairs of protein 3D structures by mean of the $C^{\alpha}(i)$–$C^{\alpha}(i+n)$ distances, where n $(3 \leq n \leq 30)$ is the number of residues intercalated between the ith and the $(i+n)$th residues. A PRIDE value equal to 1 indicates the identity between the two 3D structures that are compared, while a PRIDE value equal to 0 is associated with a pair of structures completely different.

On average, the comparison of a CH domain of type X ($X=1$, 2, 3) with another CH domain of type X results in a PRIDE value that is higher than that obtained by comparing a CH domain of type X with one of type Y ($Y \neq X$). For example, the comparison of two domains of type 1 results in an average PRIDE value of 0.560, the comparison of two domains of type 2 is associated with an average PRIDE of 0.593, while the comparison of a CH domain of type 1 and a CH domain of type 2 results in an average, lower PRIDE of 0.416. Low PRIDE values are also obtained, on average, when the CH domain of type 3 is compared with the CH domains of type 1 (0.402) and of type 2 (0.493). This clearly

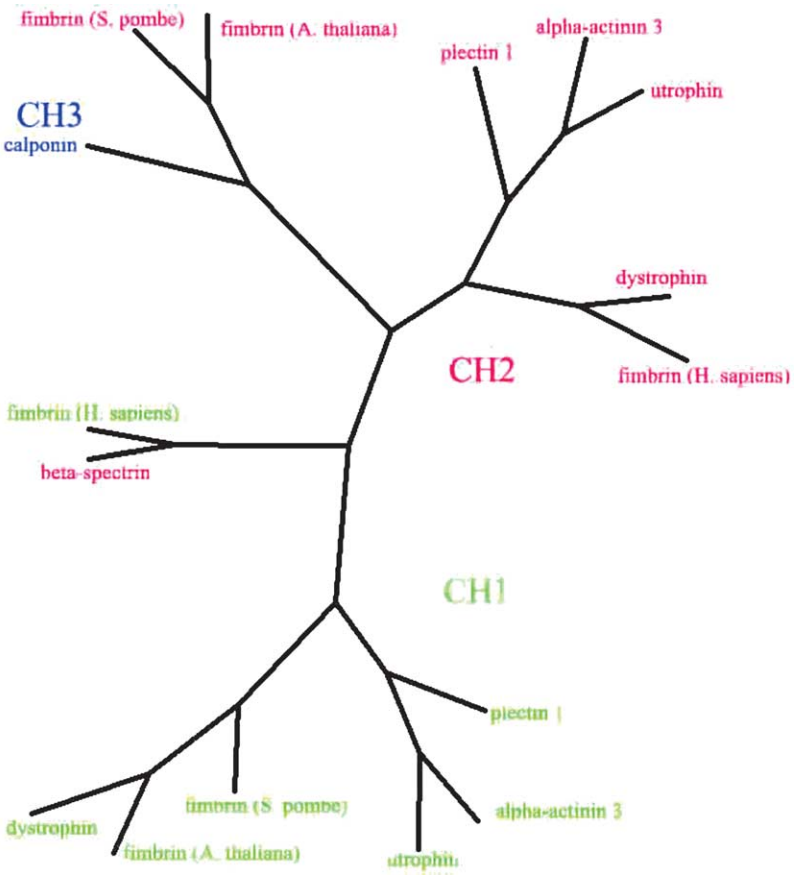

Figure 3. Dendrogram showing the classification of CH domains on the basis of their 3D structure.

indicates that the intra-similarity, that is the similarity between CH domains belonging to the same sequence class, is larger than the inter-similarity, that is, the similarity between two CH domains belonging to two different sequence groups.

This result is supported by a cluster analysis, performed with the UMPGA clustering criterion and with the Kitsch program of the Phylip software suite†. The input 16×16 square matrix **P** was built with the PRIDE values. Each element p_{ij} of the matrix indicates the distance, measured as 1-PRIDE, of the *i*th and *j*th CH domain structure. As shown in Figure 3, the CH domains of type 1 tend to cluster together and tend to be separated from the CH domains of type 2. The only exception is the CH domain of human fimbrin, which apparently is quite similar to the β-spectrin CH domain. Nevertheless, the clustering is evident, suggesting that a natural and genuine clustering of the CH domain structures is possible. Surprisingly, the only example of a CH domain of type 3 clusters with the CH domains of type 2, and is well separated from the CH domains of type 1.

Although there is a clear distinction between different classes of CH domains at the level of amino acid sequence[36,37] they have hitherto been considered to be structurally nearly identical.[15] The CH domain structurally evolved and diverged to best serve their functions. In the case of the two consecutive CH domains that form the ABD, the CH1 hosts the function of actin filament binding in two locations, while the PtdIns(4,5)P_2 and a minor actin binding site resides in CH2. The actin binding sites are located on the principal α-helices (A, G, A″). A parallel driving force towards structural diversity between CH domains is the formation of the compact domain interface, which again involves the distinct principal α-helices (A, G, G″) (Figure 1(c)). Their structure certainly underwent fine structural tuning in order to form an extensive domain interface. Similarly, these structural constraints are not present in proteins with a single CH domain (calponin), allowing therefore the development of a different CH domain structure.

Actin binding site

Several studies using mutagenesis, crosslinking and spectroscopy implicated residues that are located in different parts of the ABD domain to bind to actin filaments. Actin binding domains from several proteins of the spectrin superfamily (α-actinin, dystrophin, ABP-120, filamin) were studied to map the residues involved in interactions with actin filaments.[38–45] Three actin binding sites (ABS1–3) consistently emerge and map to the N-terminal A helix of CH1 (residues 48–57), the C-terminal G helix of CH1 (residues 123–147) and the N-terminal

† http://evolution/genetics.washington.edu/phylip.html

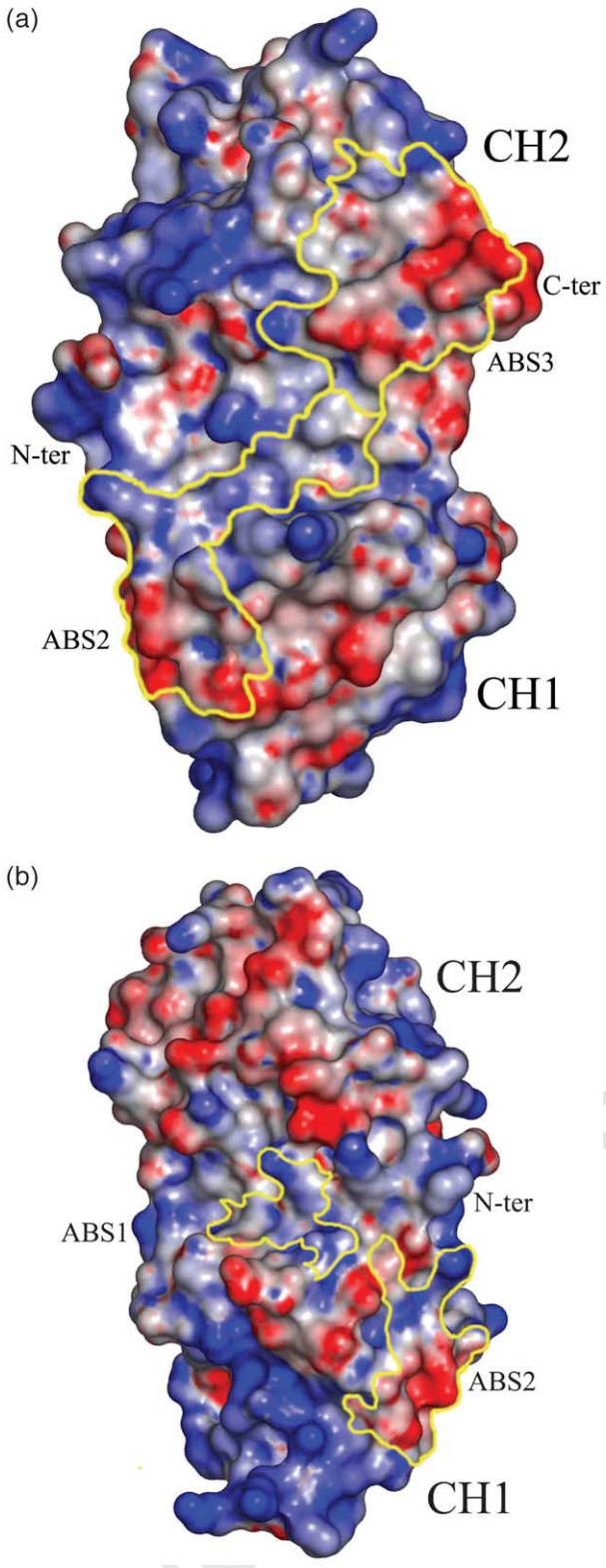

Figure 4. (a) Actin binding sites 2 and 3 mapped on the solvent-accessible surface of the α-actinin ABD colored by the electrostatic potential. Positive potential at the surface is indicated by blue, negative potential is indicated in red. Actin binding sites 2 and 3 (C-terminal helix of CH1 and N-terminal segment of CH2 domain) are delineated on the surface with a yellow line. The Figure was prepared by PyMOL. (b) Actin binding sites 1 and 2 mapped on the solvent-accessible surface of the α-actinin ABD and colored by the electrostatic potential. Positive potential at the surface is indicated in blue, negative potential is indicated in red. Actin binding sites 1 and 2 (N-terminal segment of CH1domain and C-terminal helix of CH1) are delineated on the surface with a yellow line. The Figure was prepared by PyMOL.

segment of CH2 domain (residues 153–172), comprising helix A″ (Figure 1(a)).

Biochemical characterisations of the CH1 and CH2 domains from utrophin, dystrophin, β-spectrin and α-actinin showed that the two domains are not functionally equivalent.[36,46,47] In contrast to the complete actin binding region, the isolated CH2 domain from β-spectrin does not bind to actin filaments with significant affinity. Conversely, a construct corresponding only to the CH1 domain of α-actinin does bind to actin filaments.[46] A mutagenesis study identified residues within the C-terminal part of the α-actinin CH1 domain that may be involved in binding to actin filaments, since their substitution with alanine abolishes the interaction.[45] These amino acid residues are mostly hydrophobic, which is in agreement with the accepted paradigm that the force driving the interaction with actin filaments is at least partly hydrophobic.[46]

Mapping the amino acid residues of ABS1–3 to the α-actinin ABD domain shows that ABS2 and ABS3 form a contiguous region on the surface of the domain (Figure 4(a)), while ABS1 remains, in part, buried in the interface between the two tandem CH domains in the closed conformation (Figure 4(b)). The ABS3 region encompasses the majority of the linker connecting the two CH domains and the N-terminal helix of the CH2. Since ABS1 is (partially) buried in the native closed conformation, the CH domains are expected to rearrange upon binding to actin filaments, in a way similar to that proposed for plectin.[15] This rearrangement would involve a disruption of the interaction between the two CH domains and a change of the structure of the loop connecting the two CH domains. This loop is in spatial proximity to the C-terminal part of the CH2 domain, implying that it could be close to the linker (also termed neck) between the ADB and the first spectrin-like repeat of the α-actinin molecule. In the functional α-actinin dimer, the neck binds to the CaM domain of the second subunit. This suggests that the rearrangement of the two CH domains upon binding to actin filaments could be regulated by the interaction with the CaM domain. It is possible that the CaM domain, while bound to the α-actinin neck, hinders the rearrangement of the CH1 and CH2 domains. Withdrawing Ca^{2+} or adding PtdIns(4,5)P_2 will disturb this interaction, remove the CaM, and release the CH domain, leading to increased binding of α-actinin to actin filaments and also liberating the CaM domain for interaction with titin Z-repeats or related ligands.

Table 3. List of unique protein structures in complex with PtdIns(4,5)P_2 and PtdIns(3,4,5)P_3

pdb code	lipid ligands	domain	Lipid
1B55	Kx5Kx7Kx1R	PH	PIP3
1FAO	Kx8Rx1Rx12Kx37R	PH	PIP3
1FGY	Kx8Rx1Rx20Kx37R	PH	PIP3
1H10	Kx8Rx1Rx60R	PH	PIP3
1MAI	Kx1Kx7Rx6K	PH	PIP2
1BTN	Kx12R	PH	PIP2
1HFA	Kx9Kx1K	CALM-N	PIP2
1DJX	Kx1Kx108R	PLC-D1	PIP2
1GC6	Kx2Kx214K	FERM	PIP2
1HOA	RRx2Kx13Rx37Rx5K	ENTH	PIP2
1N4K	Rx3Rx239Kx2Rx56R	I3P-RBC	PIP2
1NU2	Kx30Rx5Kx41Rx17K	PTB	PIP2

The amino acid sequence pattern of positively charged residues involved in binding is reported. Ligands within 4.5 Å distance from the phosphoinositol moiety are highlighted. Abbreviations: PH, pleckstrin homology domain; CALM-N, N-terminal domain of clathrin assembly lymphoidmyeloid leukaemia protein; PLC-D1, phosphoinositide-specific phospholipase c-delta1; FERM, Protein 4.1, Ezrin, Radixin, Moesin domain; ENTH, epsin N-terminal homology domain; I3P-RBC, inositol 1,4,5-trisphosphate receptor binding core; PTB, disabled-1 (dab1) ptb domain-apoer2 peptide. PIP2, phosphoinositol-4,5-bisphosphate; PIP3, phosphoinositol-3,4,5-trisphosphate.

PtdIns(4,5)P_2 binding site

Binding of PtdIns(4,5)P_2 was shown to regulate the filamentous actin bundling activity[48–50] as well as to activate the binding to the Z-repeats of titin,[6] by relieving the CaM domain of one α-actinin molecule from the linker between ABD and the rod of the adjacent subunit. In the "titin-free" conformation, the C-terminal CaM of one subunit of the antiparallel α-actinin dimer interacts with a short segment linking the rod to the ABD of the opposite subunit. This interaction is disrupted upon binding of PtdIns(4,5)P_2 to the ABD, releasing the CaM for binding to titin Z-repeats. Fraley *et al*. additionally investigated the role of the position of the phosphate groups of phosphatidylinositol and concluded that the phosphate groups at positions 4 and 5 interact with the α-actinin.[49] The PtdIns(4,5)P_2 binding site was mapped to a 17 amino acid residues long stretch (seq. 172–188, Figure 1(a)) of the CH2 domain (TAPYRNVNIQNFHISWK),[5,49] mapping to the loop connecting α-helices A″ and B″. Systematic inspection of the PtdIns(4,5)P_2 and PtdIns(3,4,5)P_3 ligands, as observed in all structures present to date in the PDB database (Table 3), shows that phosphate groups at positions 4 and 5 are bound to the protein moiety by least three ligands (within 4.5 Å) which are either Arg or Lys, with two of them close in sequence (from one to five amino acid in between (exception 1BTN)), and the third ligand further away in sequence. The average relative solvent accessibility of the polar side-chain atoms of Arg or Lys ligands is 41(±16)% (calculated with NACCESS program suite†) after removing PtdIns(4,5)P_2 from the structures) and the average distance between their C^{β} atoms is 11.7(±4.5) Å. The amino acid stretch predicted to be involved in binding of α-actinin to PtdIns(4,5)P_2 hosts only one Arg and one Lys residue, at positions 176 and 188, respectively. The Lys188 residue is almost buried in the protein (relative solvent accessibility of the polar side-chain atoms are 1.5%), having a structural role by forming hydrogen bonds to the carbonyl oxygen atoms of Ile241, Val242, and Thr244. This observation prompted us look for other possible ligands and we identified Arg170 (which is just outside the previously mapped region), Arg176 (within the originally defined region) and Arg199 as possible PtdIns(4,5)P_2 ligands (Figure 5). These three amino acid residues follow the pattern observed in phospholipid headgroup binding structures, their average relative solvent accessibility of the polar side-chain atoms is 53% and their average C^{β} distances are 12 Å, forming a suitable platform for PtdIns(4,5)P_2 binding. This triad of positively charged residues is present only in the CH2 domains of α-actinin isoforms[37]. The amino acid residues proposed to be involved in PtdIns(4,5)P_2 binding map to a region flanking the ABS3 site in the primary sequence as well as in the 3D structure (Figure 5).

† http://wolf.bms.umist.ac.uk.naccess/

Conclusions

The cytoskeleton consists of a number of filamentous systems composed of polymers of actin, tubulin and intermediate filament proteins. An important family of cytoskeletal proteins crosslink or bundle actin filaments. The major F-actin crosslinking protein in both muscle and non-muscle cells is α-actinin. The actin binding domain of human muscle α-actinin-3 is formed by two consecutive calponin homology domains that are arranged in the closed conformation in the native apo-form.

The conservation of the CH1–CH2 interface in the ABD domains of α-actinin (observed in the three crystallographically independent molecules in two crystal forms grown under different conditions), fimbrin, plectin, utrophin and dystrophin, as well as amino acid sequence conservation of residues

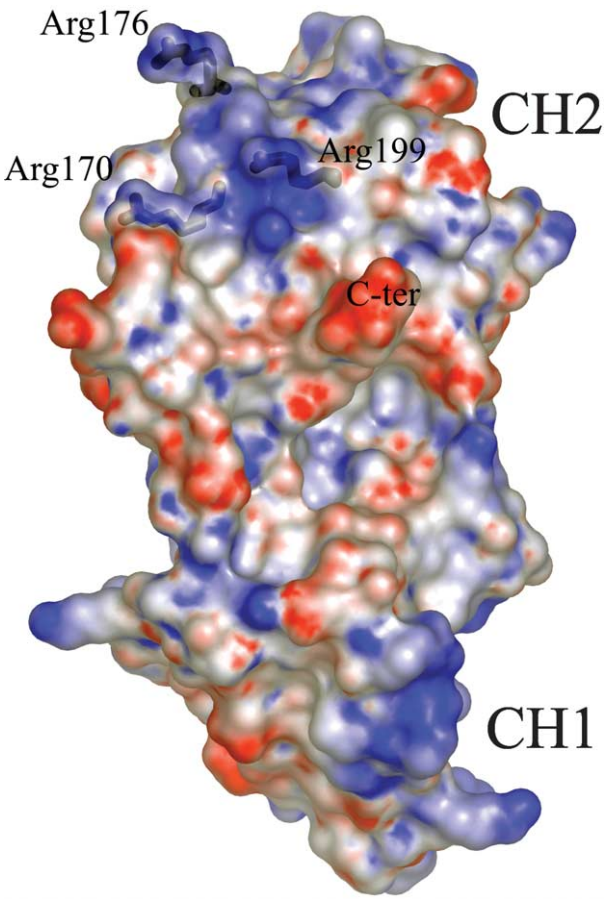

Figure 5. Electrostatic potential mapped on the solvent-accessible surface of the α-actinin ABD together with putative PtdIns(4,5)P_2 binding residues. Positive potential at the surface is indicated in blue, negative potential is indicated in red. Residues identified as putative PtdIns(4,5)P_2 ligands (170, 176, 199) are highlighted. The Figure was prepared by PyMOL.

involved in intimate contacts between the two tandem CH domains,[36] and recent cryo-EM analyses[34] suggest that the native apo-structure of the ABD of α-actinin adopts a closed conformation. Taken together, the currently available structural and biochemical information on ABDs indicates an inherent structural flexibility between the tandem CH domains. This structural plasticity allows the conformational changes that are needed for efficient binding to actin filaments, making the actin binding sites fully available to the binding partner.

Binding of PtdIns(4,5)P_2 in the proposed location (Figure 5) would orient the fatty acid moiety in a direction which allows it to interact with the linker sequence between the ABD and the first spectrin-like repeat, regulating thereby the binding of the CaM domain to this linker as suggested earlier.[6] This proposed arrangement is in agreement with observations that the phospholipid headgroup alone is insufficient to activate titin binding, and that the lipid moiety is required for full activation.

Experimental Procedures

Protein preparation, crystallisation and titin binding

The actin binding domain of α-actinin-3 (residues 26–273, Swissprot entry Q08043) was cloned into a modified pET vector with an N-terminal His_6-tag and with a TEV-protease cleavage site. Protein expression was carried out in BL21[DE3] cells at 30° C for six hours after induction at A_{600} 0.5 with 0.1 mM IPTG and gave a yield of ca 15 mg/l of culture. After affinity purification on a Ni-NTA matrix (Qiagen), the protein was cleaved with TEV protease at a ratio of 1:100 (w/w) overnight, and purified further by anion-exchange chromatography on a monoQ column (Amersham). matrix-assisted laser desorption/ionization time-of-flight (MALDI-TOF) mass spectrometry confirmed the expected mass of the protein.

The purified protein was then dialyzed to 20 mM Tris–HCl (pH 8.0) and concentrated to 17 mg/ml for crystallization. Two crystal forms were grown readily using vapour diffusion at 20° C by mixing the protein in a 1:1 volume ratio with a solution containing 8% (w/v) PEG 20000 (Fluka), 50 mM sodium acetate (pH 5.0), (crystal form H) or 30% (w/v) PEG 4000 (Fluka), 100 mM sodium cacodylate, 200 mM sodium acetate (pH 6.5) (crystal form L). Crystals in both cases were rod-shaped and had dimensions of up to 0.5 mm.

Binding of α-actinin-3 to titin Zr7 in a GST-pulldown assay. GST-Zr7 was immobilized to glutathione beads, which were washed in binding buffer (20 mM Hepes (pH 7), 50 mM NaCl, 1 mM DTT) and incubated with recombinant α-actinin-3 at 8 μM essentially as described.[6] Phospholipids (phosphatidyl-inositol 4,5-bisphosphate PtdIns(4,5)P_2, and lysophosphatidic acid) were prepared at 1 mg/ml in 0.5% (v/v) Triton X-100 solutions in binding buffer and diluted to 25 μM working concentrations in the same buffer. After incubation for 30 minutes on ice, the beads were washed by five volumes of binding buffer, and eluted with Laemmli SDS sample buffer by heating to 95 °C for five minutes and analysed by SDS-PAGE.

Data collection and structure determination

Crystals of form H were harvested in stabilization buffer containing 8% PEG 20000 (Fluka), 50 mM sodium acetate (pH 5.0), 15% (v/v) glycerol and flash-frozen in a liquid nitrogen-cooled stream. Crystals belong to space group $P1$, with unit cell dimensions of a=38.50 Å, b=45.96 Å, c=66.70 Å, α=86.7°, β=87.8°, γ=87.3°, and contain two ABD molecules in the asymmetric unit with a solvent content of approximately 41% (v/v). Diffraction data for the H crystal form were collected to 1.55 Å resolution on the wiggler beamline of the synchrotron source at Sincrotrone Trieste (Elettra), Italy, using the 345 mm MAR image plate detector (λ=1.0 Å). A single crystal was used to record the

entire data set in one sweep. Data were integrated and reduced with the DENZO/SCALEPACK programs,[51] while subsequent manipulations of diffraction data were performed using the CCP4 suite of programs (Table 1).[52]

Crystals of the L form were harvested in the reservoir solution and flash-frozen in a liquid nitrogen-cooled stream. Crystals grew in space group $P2_1$ with cell dimensions $a=46.31$ Å, $b=38.54$ Å, $c=65.48$ Å, $\beta=99.7°$, and contain one molecule per asymmetric unit, corresponding to solvent content of about 40% (v/v). Diffraction data to 2.19 Å resolution were collected on a GX-21 rotating anode generator (Elliot-Marconi Avionics) at EMBL-Heidelberg, Germany, using the 345 mm MAR image plate detector ($\lambda=1.54178$ Å). All data processing and scaling was done with XDS (Table 1).[53]

The structure of the N-terminal actin binding domain of α-actinin was solved by molecular replacement. The search models were derived from crystal structures of utrophin[16] and β-spectrin.[20] CH1 domain from utrophin (PDB code 1QAG) and CH2 domain (PDB code 1BKR) from β-spectrin were used as templates throughout the molecular replacement calculations. Attempts to use entire actin binding domains from utrophin, dystrophin or fimbrin proved to be unsuccessful. All molecular replacement calculations were performed using the program AMoRe.[54] Diffraction data of crystal form L with one molecule per asymmetric unit were firstly used for molecular replacement calculations. Two major peaks corresponding to two CH domains in the asymmetric unit were observed. The models were re-oriented according to the solutions of the cross-rotation search and used in a subsequent translational search, followed by rigid body refinement. This resulted in an *R*-factor of 45.4% and correlation coefficient of 0.345 for the diffraction data from 10–3.5 Å. This model, consisting of one CH1 and one CH2 domain per asymmetric unit was used to calculate the $2F_o-F_c$ and F_o-F_c electron density maps with the diffraction data between 30 Å and 2.5 Å. The inspection of the difference Fourier maps clearly indicated the part of the linker that connects both CH domains into a single polypeptide chain. The initial $2F_o-F_c$ map was of good quality and allowed us to rebuild most of the molecular model according to the sequence of human α-actinin isoform 3 using program O.[55] Refinement of the model by CNS[56] utilized the native dataset (Table 1), with the maximum likelihood target function.[57] Corrections for the bulk solvent were applied during the refinement. Weighting schemes,[58] as implemented in CNS, were used throughout for map calculations. The model was refined with progressive increase of the outer resolution limit; final model adjustments involved correcting errors in the side-chain conformation and locating solvent molecules. Several cycles of model building, and refinement were performed to produce the final refined model, at 2.19 Å resolution, with a crystallographic *R* value of 22.7%, a free *R* value of 27.3% (Table 1). This model consists of residues 42–265 of the human skeletal muscle α-actinin-3 and 193 water molecules. No clear electron density is observed for 41 residues at the N terminus and 12 residues at the C terminus section of the polypeptide. PROCHECK[59] was used to gauge the stereochemical quality of the final model, which scores as expected at 2.19 Å resolution. The Ramachandran plot[60] has 90.5% of the residues lying in the most-favoured regions, 8.3% in allowed regions and 1.2% in generously allowed regions. Refined overall temperature factors of 17.8 $Å^2$ (14.0 $Å^2$ for main-chain atoms, 16.3 $Å^2$ for side-chain atoms, and 27.0 $Å^2$ for water molecules) are consistent with the 25.4 $Å^2$ overall thermal factor obtained from Wilson scaling of the diffraction data.

The refined model of crystal form L was subsequently used for molecular replacement calculations to solve structure of the form H. Data in the resolution range 10–3.2 Å were used for the cross-rotation function search. Two major peaks corresponding to two ABD molecules in the asymmetric unit were observed. The model was re-oriented according to the solutions of the cross-rotation search and used in a subsequent translational search, followed by rigid body refinement of the two molecules. This resulted in an *R*-factor of 41.8% and correlation coefficient of 0.423 for the diffraction data between 10 Å and 3.2 Å. The model was refined following a protocol similar to that used for the L crystal form. Several cycles of model building, and refinement were performed to produce the final refined model at 1.6 Å resolution, with a crystallographic *R* value of 18.2% and a free *R* value of 20.8% (Table 1). The model consists of two molecules, corresponding to residues 40–266, and 41–268 of human skeletal muscle α-actinin-3, and 459 solvent molecules. No clear electron density was observed for 39/40 residues (molecules A/B) at the N terminus and (11/9) (molecules A/B) residues at the C terminus. The quality of the final model was assessed with the PROCHECK program package.[59] The final model has 88.7% of residues in the core, 10.3% in the additionally allowed and 1.0% in generously allowed regions of the Ramachandran plot.[60] Refined overall temperature factors of 19.6 $Å^2$ (17.0 $Å^2$ for main-chain atoms, 19.8 $Å^2$ for side-chain atoms, and 29.2 $Å^2$ for water molecules) are consistent with the 17.4 $Å^2$ overall thermal factor obtained from Wilson scaling of the diffraction data.

Superposition of atomic models was performed with programs TOPP and LSQKAB as implemented in the CCP4 program suite.[52] The domain interactions in the actin-binding region were analyzed by the protein–protein interaction server[24]† and the Figures were prepared with PyMOL.‡ The ABD sequences were aligned with CLUSTAL W.[61]

† http://www.biochem.ucl.ac.uk/bsm/PP/server/index.html

‡ http://pymol.sourceforge.net

Comparison of CH domains

The known structures of the CH domains were compared by means of the PRIDE values, computed with locally written software that implements the PRIDE algorithm.[35] The structural classification of the CH domains was performed with a cluster analysis, by using the Kitsch program of the Phylip software suite.[36]

Accession numbers

The coordinates and structure factors have been deposited in the Brookhaven PDB as entries 1TJT and 1WKU for crystal forms L and H, respectively.

Acknowledgements

B.S. is a recipient of a post-doctoral fellowship funded by Research Training Network CYTONET (contract no. HPRN-CT-2000-00096), which also supported the work of M.G., who is a recipient of an MRC International Appointment Initiative Award. Oliviero Carugo (University of Pavia, Italy) is gratefully acknowledged for help with structural analyses of CH domains. The excellent technical assistance of Nathalie Bleimling is gratefully acknowledged.

Competing interest statement. The authors declare that they have no competing financial interests.

Supplementary Data

Supplementary data associated with this article can be found, in the online version, at doi:10.1016/j.jmb.2005.01.002

References

1. Blanchard, A., Ohanian, V. & Critchley, D. (1989). The structure and function of alpha-actinin. *J. Muscle Res. Cell Motil.* **10**, 280–289.
2. Castresana, J. & Saraste, M. (1995). Does vav bind to F-actin through a CH domain? *FEBS Letters*, **374**, 149–151.
3. Dixson, J. D., Forstner, M. J. & Garcia, D. M. (2003). The α-actinin gene family: a revised classification. *J. Mol. Evol.* **56**, 1–10.
4. Landon, F., Gache, Y., Touitou, H. & Olomucki, A. (1985). Properties of two isoforms of human blood platelet α-actinin. *Eur. J. Biochem.* **153**, 231–237.
5. Fukami, K., Sawada, N., Endo, T. & Takenawa, T. (1996). Identification of a phosphatidylinositol 4,5-bisphosphate binding site in chicken skeletal muscle α-actinin. *J. Biol. Chem.* **271**, 2646–2650.
6. Young, P. & Gautel, M. (2000). The interaction of titin and alpha-actinin is controlled by a phospholipid-regulated intramolecular pseudoligand mechanism. *EMBO J.* **19**, 6331–6340.
7. Djinovic Carugo, K., Gautel, M., Ylanne, J. & Young, P. (2002). The spectrin repeat: a structural platform for cytoskeletal protein assemblies. *FEBS Letters*, **513**, 119–123.
8. Otey, C. A. & Carpen, O. (2004). α-Actinin revisited: a fresh look at an old player. *Cell Motil. Cytoskeleton*, **58**, 104–111.
9. Faulkner, G., Lanfranchi, G. & Valle, G. (2001). Telethonin and other new proteins of the Z-disc of skeletal muscle. *IUBMB Life*, **51**, 275–282.
10. Tskhovrebova, L. & Trinick, J. (2003). Titin: properties and family relationships. *Nature Rev. Mol. Cell. Biol.* **4**, 679–689.
11. Beggs, A. H., Byers, T. J., Knoll, J. H., Boyce, F. M., Bruns, G. A. & Kunkel, L. M. (1992). Cloning and characterization of two human skeletal muscle alpha-actinin genes located on chromosomes 1 and 11. *J. Biol. Chem.* **267**, 9281–9288.
12. Young, P., Ferguson, C., Bañuelos, S. & Gautel, M. (1998). Molecular structure of the sarcomeric Z-disk: two types of titin interactions lead to an asymmetrical sorting of α-actinin. *EMBO J.* **17**, 1614–1624.
13. Gautel, M., Goulding, D., Bullard, B., Weber, K. & Fürst, D. O. (1996). The central Z-disk region of titin is assembled from a novel repeat in variable copy numbers. *J. Cell Sci.* **109**, 2747–2754.
14. Luther, P. K. & Squire, J. M. (2002). Muscle Z-band ultrastructure: titin Z-repeats and Z-band periodicities do not match. *J. Mol. Biol.* **319**, 1157–1164.
15. Garcia-Alvarez, B., Bobkov, A., Sonnenberg, A. & de Perda, J. M. (2003). The structural and functional analysis of the actin binding domain of plectin suggest alternative mechanisms for binding to f-actin and integrin β4. *Structure*, **11**, 615–625.
16. Keep, N. H., Winder, S. J., Moores, C. A., Walke, S., Norwood, F. L. M. & Kendrick-Jones, J. (1999). Crystal structure of the actin-binding region of utrophin reveals a head-to-tail dimer. *Structure*, **7**, 1539–1546.
17. Norwood, F. L. M., Sutherland-Smith, A. J., Keep, N. H. & Kendrick-Jones, J. (2000). The structure of the N-terminal actin-binding domain of human dystrophin and how mutations in this domain may cause Duchenne or Becker muscular dystrophy. *Structure*, **8**, 481–491.
18. Goldsmith, S. C., Pokala, N., Shen, W., Fedorov, A. A., Matsudaira, P. & Almo, S. C. (1997). The structure of an actin-cross-linking domain from human fimbrin. *Nature Struct. Biol.* **4**, 708–712.
19. Klein, M. G., Shi, W., Ramagopal, U., Tseng, Y., Wirtz, D., Kovar, D. R. *et al*. (1999). Structure of the actin crosslinking core of fimbrin. *Structure*, **6**, 999–1013.
20. Djinovic Carugo, K., Bañuelos, S. & Saraste, M. (1997). Crystal structure of a calponin homology domain. *Nature Struct. Biol.* **4**, 175–179.
21. Jones, S. & Thornton, J. M. (1996). Principles of protein–protein interactions. *Proc. Natl Acad. Sci. USA*, **93**, 13–20.
22. Olski, T. M., Noegel, A. A. & Korenbaum, E. (2001). Parvin, a 42 kDa focal adhesion protein, related to the a-actinin superfamily. *J. Cell Sci.* **114**, 525–538.
23. Schlunegger, M. P., Bennett, M. J. & Eisenberg, D. (1997). Oligomer formation by 3D domain swapping: a model for protein assembly and misassembly. *Advan. Protein Chem.* **50**, 61–122.

24. Liu, Y., Gotte, G., Libonati, M. & Eisenberg, D. (2002). Structures of the two 3D domain-swapped RNase A trimers. *Protein Sci.* **2**, 371–380.
25. Yan, Y., Winograd, E., Viel, A., Cronin, T., Harrison, S. C. & Branton, D. (1993). Crystals structure of the repetitive segments of spectrin. *Science*, **262**, 2027–2030.
26. Hanein, D., Volkmann, N., Goldsmith, S., Michon, A.-M., Lehman, W., Craig, R. *et al*. (1998). An atomic model of fimbrin binding to F-actin and its implications for filament crosslinking and regulation. *Nature Struct. Biol.* **5**, 787–792.
27. Moores, C. A., Keep, N. H. & Kendrick-Jones, J. (2000). Structure of the utrophin actin-binding domain bound to F-actin reveals binding by an induced fit mechanism. *J. Mol. Biol.* **297**, 465–480.
28. Sutherland-Smith, A. J., Moores, C. A., Norwood, F. L., Hatch, V., Craig, R., Kendrick-Jones, J. & Lehman, W. (2003). An atomic model for actin binding by the CH domains and spectrin-repeat modules of utrophin and dystrophin. *J. Mol. Biol.* **329**, 15–33.
29. Galkin, V. E., Orlova, A., VanLoock, M. S., Rybakova, I. N., Ervasti, J. M. & Egelman, E. H. (2002). The utrophin actin-binding domain binds F-actin in two different modes: implications for the spectrin superfamily of proteins. *J. Cell Biol.* **157**, 243–251.
30. Galkin, V. E., Orlova, A., VanLoock, M. S. & Egelman, E. H. (2003). Do the utrophin tandem calponin homology domains bind F-actin in a compact or extended conformation? *J. Mol. Biol.* **331**, 967–972.
31. Tang, J., Taylor, D. & Taylor, K. (2001). The three-dimensional structure of alpha-actinin obtained by cryoelectron microscopy suggests a model for Ca^{2+}-dependent actin binding. *J. Mol. Biol.* **310**, 845–858.
32. Taylor, K. A. & Taylor, D. W. (1993). Projection image of smooth muscle α-actinin from two-dimensional crystals formed on positively charged lipid layers. *J. Mol. Biol.* **230**, 196–205.
33. McGough, A., Way, M. & DeRosier, D. (1994). Determination of the α-actinin-binding site on actin filaments by cryoelectron microscopy and image analysis. *J. Cell Biol.* **126**, 433–443.
34. Liu, J., Taylor, D. W. & Taylor, K. A. (2004). A 3-D reconstruction of smooth muscle alpha-actinin by CryoEm reveals two different conformations at the actin-binding region. *J. Mol. Biol.* **338**, 115–125.
35. Carugo, O. & Pongor, S. (2002). Protein fold similarity estimated by a probabilistic approach based on C^{α}–C^{α} distance comparison. *J. Mol. Biol.* **315**, 887–898.
36. Bañuelos, S., Saraste, M. & Djinovic Carugo, K. (1998). Structural comparisons of calponin homology domains: implications for actin binding. *Structure*, **6**, 1419–1431.
37. Gimona, M., Djinović Carugo, K., Kranewitter, W. J. & Winder, S. J. (2002). Functional plasticity of CH domains. *FEBS Letters*, **20**, 98–106.
38. Bresnick, A. R., Warren, V. & Condeelis, J. (1990). Identification of a short sequence essential for actin binding by Dictyostelium ABP-120. *J. Biol. Chem.* **265**, 9236–9240.
39. Bresnick, A. R., Janmey, P. A. & Condeelis, J. (1991). Evidence that a 27-residue sequence is the actin-binding site of ABP-120. *J. Biol. Chem.* **266**, 12989–12993.
40. Corrado, K., Mills, P. L. & Chamberlain, J. S. (1994). Deletion analysis of the dystrophin-actin binding domain. *FEBS Letters*, **344**, 255–260.
41. Levine, B. A., Moir, A. J. G., Patchell, V. B. & Perry, S. V. (1990). The interaction of actin with dystrophin. *FEBS Letters*, **263**, 159–162.
42. Levine, B. A., Moir, A. J., Patchell, V. B. & Perry, S. V. (1992). Binding sites involved in the interaction of actin with the N-terminal region of dystrophin. *FEBS Letters*, **298**, 44–48.
43. Fabbrizio, E., Bonet Kerrache, A., Leger, J. J. & Mornet, D. (1993). Actin–dystrophin interface. *Biochemistry*, **32**, 10457–10463.
44. Kuhlman, P. A., Hemmings, L. & Critchley, D. R. (1992). The identification and characterisation of an actin binding site in α-actinin by mutagenesis. *FEBS Letters*, **304**, 201–206.
45. Lebart, M.-C., Méjean, C., Casanova, D., Audemard, E., Derancourt, J., Roustan, C. & Benyamin, Y. (1994). Characterization of the actin binding site on smooth muscle filamin. *J. Biol. Chem.* **269**, 4279–4284.
46. Way, M., Pope, B. & Weeds, A. (1992). Evidence for functional homology in the F-actin binding domains of gelsolin and α-actinin: implications for the requirements for severing and capping. *J. Cell. Biol.* **119**, 835–842.
47. Winder, S. J. & Walsh, M. P. (1996). Calponin. *Curr. Top. Cell. Regul.* **4**, 33–61.
48. Fukami, K., Furuhashi, K., Inagaki, M., Endo, T., Hatano, S. & Takenawa, T. (1992). Requirement of phosphatidylinositol 4,5-bisphosphate for alpha-actinin function. *Nature*, **359**, 150–152.
49. Fraley, T. S., Tran, T. C., Corgan, A. M., Nash, C. A., Hao, J., Critchley, D. R. & Greenwood, J. A. (2003). Phosphoinositide binding inhibits α-actinin bundling activity. *J. Biol. Chem.* **278**, 24039–24045.
50. Corgan, A. M., Singleton, C., Santoso, C. B. & Greenwood, J. A. (2004). Phosphoinositides differentially regulate alpha-actinin flexibility and function. *Biochem. J.* **378**, 1067–1072.
51. Otwinowski, Z. & Minor, W. (1997). Processing of X-ray diffraction data collected in oscillation mode. *Methods Enzymol.* **276**, 307–326.
52. Collaborative Computing Project Number 4 (1994). The CCP4 suite: programs for protein crystallography. *Acta Crystallog. sect. D*, **50**, 760–763.
53. Kabsch, W. (1993). Automatic processing of rotation diffraction data from crystals of initially unknown symmetry and cell constants. *J. Appl. Crystallog.* **26**, 795–800.
54. Navaza, J. (1994). AMoRe: an automated package for molecular replacement. *Acta Crystallog. sect. A*, **50**, 157163.
55. Jones, T. A., Cowan, S., Zou, J.-Y. & Kjeldgaard, M. (1991). Improved methods for building protein models in electron density maps and the location of errors in these models. *Acta Crystallog. sect. A*, **47**, 110–119.
56. Bruenger, A. T. (1998). Crystallography and NMR systems: a new software suite for macromolecular structure determination. *Acta Crystallog. sect. D*, **54**, 905–921.
57. Pannu, N. S. & Read, R. J. (1996). Improved structure refinement through maximum likelihood. *Acta Crystallog. sect. A*, **52**, 659–668.
58. Read, R. J. (1986). Improved Fourier coefficients for maps using phases from partial structures with errors. *Acta Crystallog. sect. A*, **42**, 140–149.
59. Laskowski, R. A., MacArthur, M. W., Moss, D. S. & Thornton, J. M. (1993). PROCHECK: a program to check the stereochemical quality of protein structures. *J. Appl. Crystallog.* **26**, 283–291.

60. Ramachandran, G. N. & Sasisekharan, V. (1968). Conformation of polypeptides and proteins. *Advan. Protein Chem.* **23**, 283–437.
61. Thompson, J. D., Higgins, D. G. & Gibson, T. J. (1994). CLUSTAL W: improving the sensitivity of progressive multiple sequence alignment through sequence weighting, positions-specific gap penalties and weight matrix choice. *Nucl. Acids Res.* **22**, 4673–4680.

Edited by R. Huber

(Received 12 August 2004; received in revised form 22 December 2004; accepted 3 January 2005)